DEVELOPMENT OF A 3-D EDDY CURRENT MODEL FOR NONDESTRUCTIVE TESTING PHENOMENA*

N. Ida

Electrical Engineering Department
Colorado State University
Fort Collins, CO 80523

INTRODUCTION

The success of two-dimensional eddy current models for modeling a variety of important nondestructive testing situations has been reported elsewhere[1-3]. These models, based on the finite element method, are limited to two-dimensional and axisymmetric geometries but, nevertheless are quite capable of providing important data for many practical test geometries which can be approximated by 2-D or axisymmetric formulations. The general NDT problem, is, however, a true three-dimensional problem and must be modeled as such. A 3-D eddy current model is, therefore, a natural and obvious extension of the 2-D modeling capabilities available today. Such a model is particularly valuable since the interaction between applied fields, induced currents and complicated material discontinuities cannot be described by closed form equations nor can they be approximated by 2-D geometries. In addition, such situations cannot be replicated experimentally and, therefore, the numerical model is in many cases the only practical way to provide training data for signal processing equipment and algorithms and indeed, the only way to determine defect characterization parameters to aid in the design of eddy current probes and testing equipment.

The model described here is based on the finite element formulation of the basic Maxwell equations in differential form and, therefore, is applicable to any electromagnetic problem within the

*This work was supported by the Electric Power Research Institute under project RP 1395-2.

assumptions made in the formulation. It has many characteristics in common with a previously reported magnetostatic model[4] including efficient off-core solution routines.

ELECTROMAGNETIC FIELD EQUATIONS

The differential equations governing the general time varying fields in regions that include magnetic and conducting materials can be derived from the Maxwell equations

$$\nabla X\bar{E} = -\frac{\partial \bar{B}}{\partial t} \tag{1}$$

$$\nabla X\bar{H} = \bar{J} \tag{2}$$

$$\nabla .\bar{B} = 0 \tag{3}$$

$$\nabla .\bar{D} = 0 \tag{4}$$

where the displacement current in Eq. (2) and the volume charge in Eq. (4) are neglected. By substituting the constitutive relations $\bar{B}=\mu\bar{H}$, $\bar{J}=\sigma\bar{E}$ together with the definition of the magnetic vector potential $\bar{B}=\nabla X\bar{A}$ and denoting $\nu=1/\mu$ one reaches the curl-curl equation

$$\nu\nabla X(\nabla X\bar{A}) = -\frac{\partial \bar{A}}{\partial t} - \sigma\nabla\Phi \tag{5}$$

The permeability and conductivity are assumed to be linear (no dependence of permeability on the field or of conductivity on either applied or induced currents). Spatial variations in both μ and σ are allowed as long as these are constant in each direction of each element. The inclusion of the magnetic scalar potential Φ in Eq. (5) assures a nonvanishing electrical field for static problems. Since the only possible source for the electrical field is the applied current desity, $-\sigma\nabla\Phi$ can be replaced by J_s. In addition, for sinusoidal excitation (steady state), the magnetic vector potential is a phasor quantity therefore its time derivative can be written as

$$\frac{\partial \bar{A}}{\partial t} = -j\omega\bar{A} \tag{6}$$

Eq. (5) can now be written as

$$\nu\nabla X(\nabla X\bar{A}) = -j\omega\sigma\bar{A} + \bar{J}_s \tag{7}$$

This equation can now be solved for the three components of $\bar{A}$ from which other quantities of interest can be calculated. The solution for $\bar{A}$ is not unique unless the divergence of $\bar{A}$ is zero. This condition has not been specified explicitly in this formulation but it has been shown[5] that the choice of isoparametric finite elements for the formulation guarantees a local nondivergence of $\bar{A}$. Also, a unique solution is obtained by specifying Dirichlet boundary conditions on all the outer boundaries of the solution region[6]. This is particularly true in NDT applications where the fields are relatively tight around the sources (eddy current coils).

FINITE ELEMENT FORMULATION AND DISCRETIZATION

Instead of solving Eq. (7) directly, an energy functional, equivalent to Eq. (7) is formulated . The solution of this functional is equivalent to the solution of Eq. (7). A suitable functional can be written based on the energy balance in the solution region as

$$F(\bar{A}) = \int_V \frac{1}{2}\left[\nu \bar{B}^2 - \bar{J}_s . \bar{A} + j\omega\sigma \left|\bar{A}\right|^2 \right] dv \qquad (8)$$

where the first term represents the stored energy in the magnetic field, the second represents the input energy and the third is the dissipated energy associated with the eddy currents. The stationary point of this functional is found by taking the derivative with respect to each unknown equal to zero

$$\frac{\partial F(A)}{\partial A_{ki}} = 0 \qquad k=x,y,z \; ; \quad i=1,2,.....N \qquad (9)$$

where N is the total number of points in the solution region. The volume of interest is now discretized into a large number of 8 node hexahedral isoparametric elements. The magnetic vector potential is approximated within each element as[7]

$$A = \sum_{i=1}^{8} W_i A_i \qquad (10)$$

Substituting Eq. (10) into the energy functional and performing the derivatives in Eq. (9) yield the standard finite element equation

$$\{[S] + j[R]\}.\{A\} - \{Q\} = 0 \qquad (11)$$

where [S] is the real part of the global system of equations, [R] is the imaginary part of the system, and {Q} is a vector representing the sources in the solution region. This system of linear equations is solved for the 3N unknown values of A. Although the system in Eq. (11) is symmetric and banded the space needed to store it in a computer's memory is too large for any realistic problem due to the large bandwidth associated with 3-D problems. A frontal method of assembly and elimination based on the Gauss elimination algorithm combined with a skyline storage algorithm is used[8]. This method in effect partitions the matrix into manageable sections while using a very efficient storing algorithm with little overhead.

BOUNDARY CONDITIONS

There are two types of boundaries of interest in NDT problems; symmetry (reflection) boundaries and external (Dirichlet) boundaries. Symmetry boundaries are used whenever the problem has a symmetry plane in order to minimize the number of nodes in the solution region. These are left unspecified since the values of A are not known on the boundary. Specified boundaries are the external boundaries of the solution region. In particular, whenever the outer boundaries

are taken sufficiently far from the source, zero values for the magnetic vector potential are specified. In other cases, the boundary conditions (Dirichlet type) can be calculated or are known. (Newmann type boundary conditions are implicit in the formulation)[9].

RESULTS

The method described above was first applied to an axisymmetric problem and the axisymmetric and 3-D results compared directly. The geometry of this situation is outlined in Fig. 1. It consists of an Inconel 600 tube section inside the tube sheet in a steam generator. The impedance of an absolute eddy current probe is calculated and compared to identical calculations with an axisymmetric code[1]. Fig. 2 shows the discretization of one quarter of the geometry, due to symmetry about the planes X=0 and Y=0. Other symmetry planes can be specified such as X=0 and X-Y=0. This region is discretized into 1040 elements and 1358 nodes (4074 unknowns) and the resulting system of equations solved for the three components of the magnetic vector potential at each of the nodes. From the values of A the coil impedance is calculated as follows[9]:

The stored energy in the solution region is given by

$$W = \sum_{i=1}^{N} \frac{1}{2}(\nu_x B_{xi}^2 + \nu_y B_{yi}^2 + \nu_z B_{zi}^2) \tag{12}$$

where N is the total number of elements. The inductance of the source is then calculated as

$$L = \frac{2W}{I^2} \tag{13}$$

where I is the R.M.S current in the source (coil). Similarly, the dissipated energy is found from the eddy current distribution

$$P = \sum_{i=1}^{N} \nu_i \sigma \omega^2 A_{ci}^2 \tag{14}$$

where A_{ci} is the centroidal value of A and is calculated as an average of the 8 nodal values in each element. The coil resistance is

$$R = P/I^2 \tag{15}$$

and the impedance becomes

$$Z = R + j\omega L = \frac{1}{I^2}(P + j\omega 2W) \tag{16}$$

The impedances for six different situations ranging from a coil in air to a coil in the Inconel tube at the edge of the tube sheet were calculated and are compared in Fig. 3. This figure also shows schematically the different geometries considered and the relative error of the 3-D solution compared to the axisymmetric solution. These errors stem mainly from the coarseness of the 3-D discretization and can be reduced by increasing the number of elements.

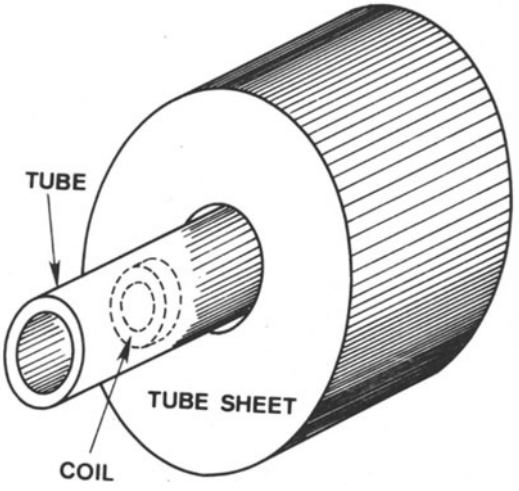

Fig. 1. An Inconel 600 tube section inside the carbon steel tube sheet.

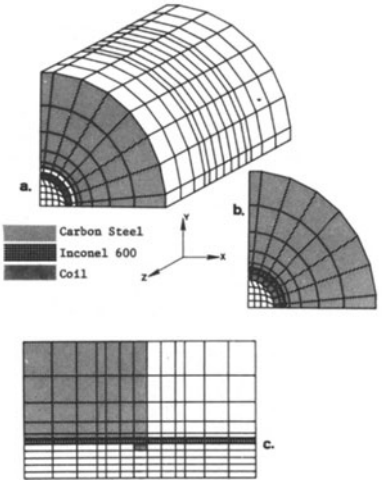

Fig. 2. Finite element discretization a) Complete mesh with hidden lines removed, b) cross section in the X-Y plane, c) cross section through the Y-Z plane at X=0.

		3-D	AXISYMMETRIC
1.	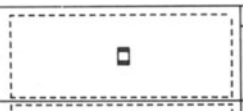	$0.0 + j0.28478\times10^{-6}$ (10.58%)	$0.0 + j0.31848\times10^{-6}$
2.	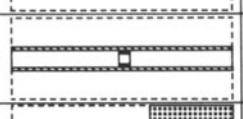	$0.16092\times10^{-6} + j0.22830\times10^{-6}$ (2.6%)	$0.15670\times10^{-6} + j0.23269\times10^{-6}$
3.	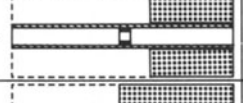	$0.20911\times10^{-6} + j0.32639\times10^{-6}$ (11.8%)	$0.18654\times10^{-6} + j0.35521\times10^{-6}$
4.	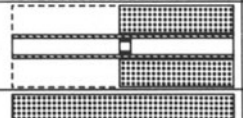	$0.18511\times10^{-6} + j0.30874\times10^{-6}$ (10.2%)	$0.16618\times10^{-6} + j0.34662\times10^{-6}$
5.	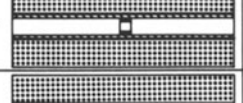	$0.23301\times10^{-6} + j0.38752\times10^{-6}$ (7.5%)	$0.24821\times10^{-6} + j0.35845\times10^{-6}$
6.	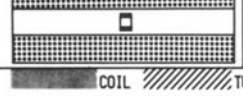	$0.55508\times10^{-7} + j0.28752\times10^{-6}$ (9.8%)	$0.50848\times10^{-7} + j0.31912\times10^{-6}$

COIL TUBE TUBE SHEET

Fig. 3. Comparison of 3-D and axisymmetric solutions for different situations. For each geometry the coil impedance is compared directly. The figures in parentheses are the errors calculated for each situation.

To demonstrate the applicability of this method to moving probe eddy current problems the geometry in Fig. 4 was considered. It consists of an Inconel tube with four square through wall holes and a differential eddy current probe operated at 1 kHz moving inside the tube. The finite element mesh (1440 elements, 1843 nodes, 5529 unknowns) is shown in Fig. 5. The coils are moved in the central portion of the mesh (Fig. 5c) and the impedance is calculated at 8 positions to produce an impedance plane trajectory characteristic of the defect encountered. This trajectory is compared in Fig. 6 with an experimental trajectory obtained from an Inconel tube with four machined holes identical to those modeled. For a problem of this kind many more probe positions are required, resulting in very large meshes but the agreement with the experimental results in Fig 6 is good considering the size of the mesh used.

CONCLUSIONS

The finite element model presented here is general and applicable to any situation involving magnetic and nonmagnetic materials. It is linear but spatial variations in permeability and conductivity can be modeled. The model was tested and compared to axisymmetric and experimental data showing consistent agreement. It is however, necessary to increase the number of elements to allow modeling of more complicated geometries with more probe positions and better accuracy. Although this can be done with the computer code as it is, the solution times involved are large and, therefore, a more drastic approach is needed. It is the intention of the author to adapt this model for solution on a CYBER-205 vector computer. This promises to allow solution of 3-D problems in times comparable to 2-D solutions.

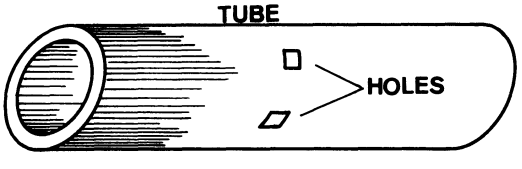

Fig. 4. An Inconel 600 tube with four square through wall holes arranged at 90°. A differential eddy current probe is moved inside to produce an impedance plane trajectory.

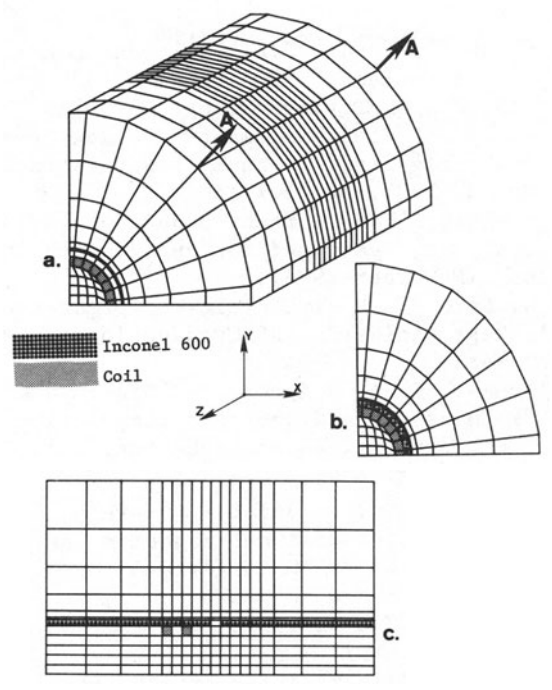

Fig. 5. Discretization of the geometry in Fig 4 into finite elements. a) complete mesh with hidden lines removed, b) cross section in the plane X-Z through one of the coils and c) cross section in the plane A-A. The probe is shown in its first position.

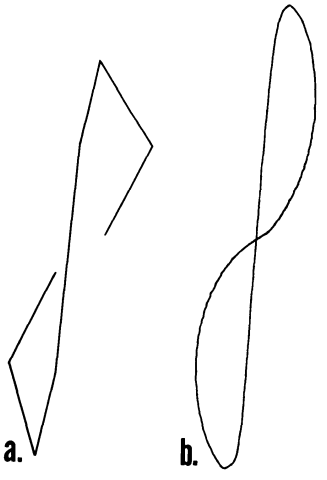

Fig. 6. Comparison of calculated and experimental impedance plane trajectories. a) finite element prediction and b) experimental impedance plane trajectory.

REFERENCES

1. R. Palanisamy and W. Lord, "Finite element modeling of electromagnetic NDT phenomena," IEEE Transactions on Magnetics, Vol. MAG-15, No. 6, Nov. 1979, pp. 1979-81.
2. N. Ida and W. Lord, "Finite elèment modeling of absolute eddy current probe signals," Journal of Nondestructive Evaluation, Vol. 3, No. 3, 1983, pp. 147-154.
3. N. Ida and W. Lord, "Eddy current probe design using finite element analysis," accepted for publication in Materials Evaluation, (November 1983).
4. N. Ida and W. Lord, "3-D finite element predictions of magnetostatic leakage fields," IEEE Transactions on Magnetics, September 1983.
5. C. S. Biddlecombe, E. A. Heighway, J. Simkin and C. W. Trowbridge, "Methods for eddy current computation in three dimensions," IEEE Transactions on Magnetics, Vol. MAG-18, No. 2, March 1982, pp. 379-399.
6. J. R. Brauer, R. Y. Bodine and L. A. Larkin, "Nonlinear anisotropic three dimensional magnetic energy functional," presented at the COMPUMAG Conference, Genoa, Italy, March 30-June 2, 1983.
7. O. C. Zienkiewicz, "The finite element method," McGraw-Hill Book Co., London, 1977.
8. E. Thompson and Y. Shimazaki, "A frontal procedure using skyline storage," International Journal for Numerical Methods in Engineering, Vol. 15, 1980, pp. 889-910.
9. N. Ida, "Three dimensional finite element modeling of electromagnetic nondestructive testing phenomena," Ph.D. Dissertation, Colorado State University, Spring, 1983.